Talanta 247 (2022) 123599

Contents lists available at ScienceDirect

Talanta

journal homepage: www.elsevier.com/locate/talanta

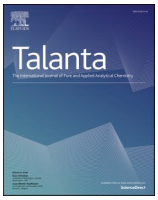

Optical fiber SPR biosensor based on gold nanoparticle amplification for DNA hybridization detection

Like Li [a], Ya-nan Zhang [a,b,c,*], Wanlu Zheng [a], Xuegang Li [a,b,c], Yong Zhao [a,b,c,**]

[a] College of Information Science and Engineering, Northeastern University, Shenyang 110819, China
[b] Hebei Key Laboratory of Micro-Nano Precision Optical Sensing and Measurement Technology, Qinhuangdao 066004, China
[c] State Key Laboratory of Synthetical Automation for Process Industries, Shenyang 110819, China

ARTICLE INFO

Keywords:
Optical fiber sensor
Biosensor
Surface plasmon resonance
Gold nanoparticles
DNA hybridization

ABSTRACT

An optical fiber SPR biosensor based on multimode fiber (MMF)- hollow core fiber (HCF)-MMF is proposed and experimentally confirmed for in situ DNA hybridization analysis. In order to improve the sensitivity of DNA hybridization detection, a sandwich model based on gold nanoparticles (AuNPs) amplification is proposed. In this model, the probe DNA (pDNA) is first modified on the optical fiber sensing area by covalent bonding, and then the biotinylated target DNA (tDNA) is modified on the AuNPs by the high affinity between biotin and streptavidin. Finally, the tDNA on the surface of the AuNPs specifically hybridizes with the pDNA on the optical fiber to form a sandwich model. The near field coupling enhancement between AuNPs and gold film and the high mass ratio of AuNPs give high sensitivity to DNA hybridization detection. Experimental results show that the sandwich-type fiber SPR sensor has a log-linear response in the DNA concentration range of 1 pM–10 nM, and the sensitivity and detection limit are 4.04 nm/log(μM) and 1pM, respectively. This is 1.44 times more sensitive than that without sandwich assay. In addition, the DNA sensor has good specificity and stability, which foreshadows its great application potential in the fields of disease diagnosis, microbial detection and environmental science.

1. Introduction

Deoxyribonucleic acid (DNA) plays a significant role in storing and transmitting genetic information to control biological development. Therefore, the specific identification and quantitative detection of DNA sequences are of great significance for accelerating the research of disease diagnosis, drug research, microbial detection, and environmental science [1–3]. Generally speaking, the detection of a specific DNA sequence is achieved through DNA hybridization, in which two single-stranded DNA (ssDNA) molecules with complementary base sequences can form a stable double-stranded DNA (dsDNA) through base pairing.

In the past few decades, many rapid and sensitive methods have been proposed for DNA hybridization detection, including electrochemistry [4,5], colorimetry [6,7], surface plasmon resonance (SPR) [8,9], surface-enhanced Raman scattering (SERS) [10,11] and optical fiber sensing [12,13]. Among all these sensing methods, optical fiber sensors have gained extensive research interest due to their advantages of anti-electromagnetic interference, small size, simple preparation, rapid response and easy integration [14,15].

So far, a large number of optical fiber DNA sensors have been proposed for DNA hybridization detection. In 2017, Guan et al. proposed a highly sensitive optical fiber DNA sensor based on the micro-fiber Sagnac interferometer, with a detection range of 100 pM to 1 μM and a detection limit of 75 pM [16]. In 2019, Zhang et al. proposed an SPR biosensor for DNA hybridization detection by modifying graphene/Au film (G/Au) on D-shape plastic optical fiber (D-POF) [17]. In 2020, Santano et al. reported an excellent review, which provided a comprehensive and systematic review of the current research status of optical fiber DNA sensors [18]. Recently, based on grapefruit microstructured optical fiber (MOF), Zhang et al. designed and prepared a whispering gallery mode (WGM) resonator, and realized label free DNA hybridization detection [19]. Among all the optical fiber biosensors, the sensors based on interferometer and SPR have higher sensitivity. However, they still have certain challenges in detecting low-concentration and small-fragment of DNA. Currently, optical fiber interferometric sensors for DNA hybridization detection are usually based on micro-nano fibers, so these sensors suffer from the disadvantage of poor mechanical

* Corresponding author. College of Information Science and Engineering, Northeastern University, Shenyang 110819, China.
** Corresponding author. College of Information Science and Engineering, Northeastern University, Shenyang 110819, China.
E-mail addresses: zhangyanan@ise.neu.edu.cn (Y.-n. Zhang), zhaoyong@ise.neu.edu.cn (Y. Zhao).

https://doi.org/10.1016/j.talanta.2022.123599
Received 4 October 2021; Received in revised form 28 March 2022; Accepted 25 May 2022
Available online 28 May 2022

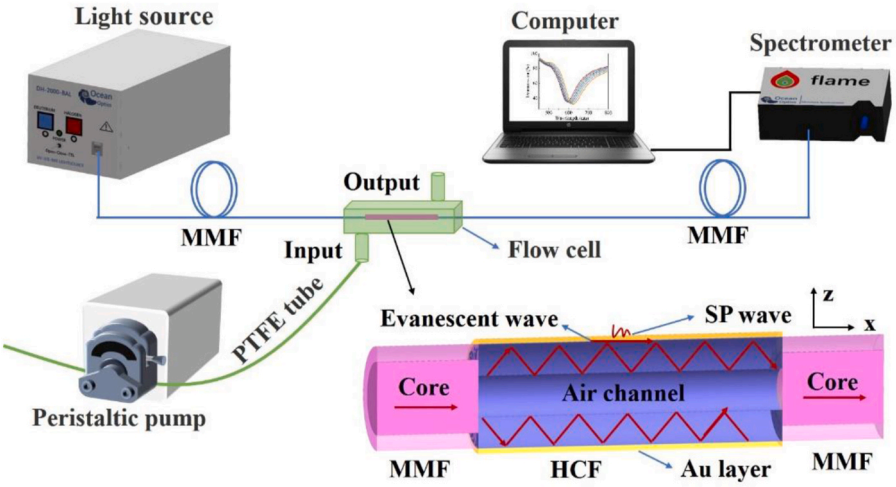

Fig. 1. Schematic of the experimental system.

strength [20–22]. Compared with them, the optical fiber SPR sensing structures have the merits of rich variety, high mechanical strength and simple preparation [23–25].

With the rapid development of nanotechnology, SPR sensors enhanced by nanomaterials are expected to the detection of low-concentration and small molecular weight biochemical analytes. In 2014, Zeng et al. systematically and comprehensively reviewed the sensitivity-enhancement methods and commonly used nanomaterials in SPR sensors, which has important guiding significance for the design and preparation of ultra-sensitive optical fiber SPR sensors enhanced by nanomaterials [26]. So far, researchers have proposed many optical fiber SPR biosensing methods enhanced by nanomaterials. Generally speaking, these methods can be divided into three types. One is to improve the immobilization efficiency of biomolecules by immobilizing some functional nanomaterials on the surface of the gold film, such as graphene oxide [27]; The second is to modify some novel two-dimensional nanomaterials on the surface of the optical fiber, such as 2D Mxene $Ti_3C_2T_X$ and MoS_2 nanosheets, to stimulate stronger SPR phenomenon [28,29]; The third is to use gold nanoparticles (AuNPs) as a signal amplification strategy, in which the electromagnetic coupling between the gold film and the AuNPs can significantly improve the detection sensitivity [30–33]. Since AuNPs are easy to be prepared and their surface are easy to be functionalized, optical fiber SPR sensors enhanced by AuNPs are a current research hotspot. For example, in 2020, Wang et al. achieved ultra-high detection sensitivity by depositing multilayer AuNPs on the surface of the gold film. This was due to the strong electromagnetic coupling between the multilayer AuNPs and the gold film [30]. However, in this method, the AuNPs directly modified on the surface of the gold film are easy to aggregate and unevenly distributed, and the AuNPs are easy to be washed away, which will affect the sensing performance. To avoid this problem, this paper proposes a smart sandwich assay based on AuNPs sensitization for DNA hybridization detection. One of the key ideas of this sensitization method is to directly modify the target DNA (tDNA) of different concentrations on AuNPs, and then detect the tDNA concentration.

In this paper, an optical fiber SPR biosensor based on AuNPs sensitized is proposed for highly sensitive DNA hybridization detection. The adopted optical fiber structure is multimode fiber (MMF)- hollow core fiber (HCF)-MMF, which has the advantages of high sensitivity, high mechanical strength, simple preparation and low cost. By immobilizing tDNA on AuNPs, and then pumping it into the sensing area to hybridize with the probe DNA (pDNA), real-time detection of tDNA and signal amplification are realized. The experimental results confirmed that the DNA detection scheme based on the sandwich assay had higher detection sensitivity than that without AuNPs sensitization. In addition, by encapsulating the optical fiber sensing structure in a microfluidic cell, the structure has the characteristics of low sample consumption and strong anti-interference ability.

2. Design and analysis

The schematic of the experimental system is shown in Fig. 1. It is mainly composed of a light source (Ocean Optics, DH-2000-bal), a spectrometer (Ocean Optics, flame), a computer, a microfluidic peristaltic pump (LongerPump, L100-1S-1) and a part of sensing structure. The sensing structure is an SPR sensing structure based on MMF-HCF-MMF. Its preparation mainly includes two steps: structure splicing and gold film plating. First, 1 cm HCF was spliced between two MMFs to obtain the MMF-HCF-MMF sensing structure. HCF has an inner diameter of 20 μm and an outer diameter of 125 μm, which can be purchased from INNSEP Co., Ltd. The MMF, with a core diameter of 105 μm and a cladding diameter of 125 μm, was purchased from YOFC Fiber Co., Ltd. In order to excite SPR effectively, a gold film of about 50 nm was sputtered on the outer surface of the HCF through a small ion sputtering apparatus (JS-1600). A beam of light from the light source is transmitted to the spectrometer through the SPR sensing structure, and then the computer displays the spectrum in real time. The optical fiber sensing structure was encapsulated in a microfluidic cell with a microfluidic inlet and outlet, and the microfluidic peristaltic pump was used to transport analytes to the microfluidic cell, which constituted a simple microfluidic system. The introduction of the microfluidic system gives the sensor the characteristics of high sensitivity, low sample consumption and immunity from external environmental factors [14,34,35].

When a beam of light from the light source is transmitted to the HCF through the MMF, most of the light beam will be transmitted in the cladding of the HCF by total internal reflection, thereby generating evanescent waves on the inner and outer surfaces of the HCF, respectively. Then, the evanescent wave can pass through the gold layer to excite surface plasmon waves (SP waves) at the interface between the gold layer and the external environment. When the wave vector of the evanescent wave is equal to the wave vector of the SP waves, SPR appears. At this time, an attenuation valley will appear at a specific wavelength of the transmission spectrum, and this specific wavelength is also known as the resonance wavelength. When the refractive index (RI) of the medium environment around the HCF changes, the position of the attenuation valley will also change, so that the RI of the external environment can be detected by tracking the movement of the attenuation valley position.

In this paper, when the tDNA is hybridized with pDNA immobilized on the HCF surface, the RI of HCF surface will change, so the optical fiber

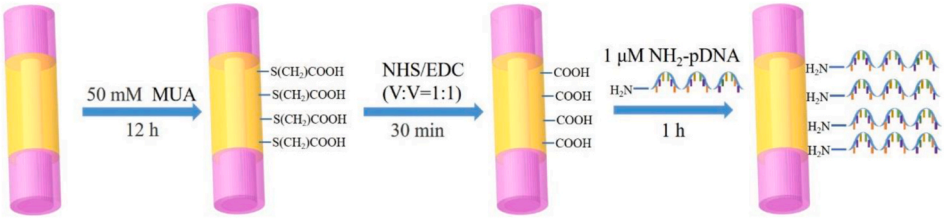

Fig. 2. Schematic of the functionalization process of pDNA on the fiber surface.

SPR sensor can be used to detect DNA hybridization.

3. Experiment

3.1. Materials and reagents

The following chemical reagents, MUA (11-Mercaptoundecanoic acid), NHS (*N*-hydroxysuccinimide) and EDC (*N*-(3-Dimethylamino-propyl)-*N*′- ethylcarbodiimide hydrochloride) were purchased from Aladdin Ltd. Streptavidin solution (1 mg/mL) was purchased from Bioss. All reagents and chemicals are of analytical grade, and no further purification is required before use. The DNA sequences used in the experiment were synthesized by Shanghai Sangon Biotechnology Co. Ltd with HPLC purification method. All DNA sequences include pDNA, tDNA, non-complementary DNA (non-cDNA), biotinylated tDNA (biotin-tDNA) and biotinylated non-complementary DNA (biotin-non-cDNA). Their base sequences are as follows:

pDNA: 5′-NH_2-CAG GAT ATG TGG CGG ATG AGC GGC A-3′

tDNA: 5′- TGC CGC TCA TCC GCC ACA TAT CCT G-3′

non-cDNA: 5′- GGC CAT CGT TGA AGA TAC CTC TGC C-3′

Biotin-tDNA: 5′-Biotin-TGC CGC TCA TCC GCC ACA TAT CCT G-3′

Biotin-non- cDNA: 5′-Biotin-GGC CAT CGT TGA AGA TAC CTC TGC C-3′

Where, tDNA is completely complementary to pDNA.

The above DNA sequences were dissolved in 10 mM phosphate buffered saline (PBS, pH = 7.2) to obtain the desired concentration of DNA solution. 50 mM MUA solution was prepared by dissolving 0.1092 g MUA in 10 mL absolute ethanol. 50 mM NHS solution was prepared by dissolving 0.0575 g NHS in 10 mL ultrapure water, and 200 mM EDC solution was prepared by dissolving 0.3834 g EDC in 10 mL ultrapure water.

3.2. Immobilization of pDNA on the optical fiber SPR sensor

To immobilize the pDNA on the sensing area to capture the tDNA, a series of functionalization steps were performed. First, the gold-coated optical fiber sensing structure was immersed in 50 mM MUA solution overnight to realize the carboxylation of the sensing surface. Then, absolute ethanol and deionized water were used to clean the non-covalently bound MUA molecules on the surface of the fiber. Next, the sensing region was immersed in an activation solution for 30 min to activate the carboxyl groups on the fiber surface. The activation solution is a mixture of 50 mM NHS solution and 200 mM EDC solution (V: V = 1:1). Similarly, deionized water was then used to rinse the fiber surface. Lastly, 1 μM aminated pDNA solution was pumped into the sensing area to achieve immobilization of pDNA through the amidation reaction between the amino group and the carboxyl group. Similarly, deionized water was then used to rinse the fiber surface to remove unbound or weakly bound pDNA. The schematic of the functionalization process is shown in Fig. 2.

3.3. Immobilization of tDNA on AuNPs

According to Refs. [36,37], the experimental procedures of immobilizing tDNA on AuNPs are as follows: (1) The AuNPs solution was first prepared by citrate reduction of $HAuCl_4$. This process has been described in detail in Refs. [38,39]. (2) 1 mL of colloidal AuNPs solution was mixed with 25 μL of streptavidin solution (1 mg/mL), and incubated at 4 °C for 1 h. (3) NaOH was adopted to adjust the pH value of the mixed solution to 8.5. (4) The mixed solution was incubated overnight at 4 °C. (5) To remove the streptavidin molecular unmodified on AuNPs, the above mixed solution was centrifuged at 9000 rpm for 20 min. Then the supernatant was removed, and the precipitate was resuspended in different concentrations of biotin-tDNA solution. (6) The above solution was incubated at 4 °C for 30 min to ensure that the biotin-tDNA was fully bound to the AuNPs modified with streptavidin. (7) The above solution

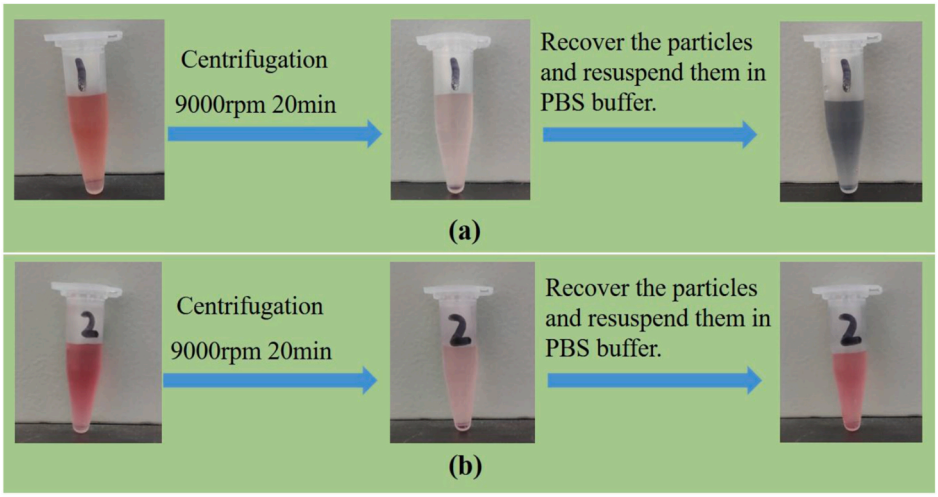

Fig. 3. Two groups of control experiments: (a) naked AuNPs solution; (b) mixed solution of strepavidin and AuNPs after incubation.

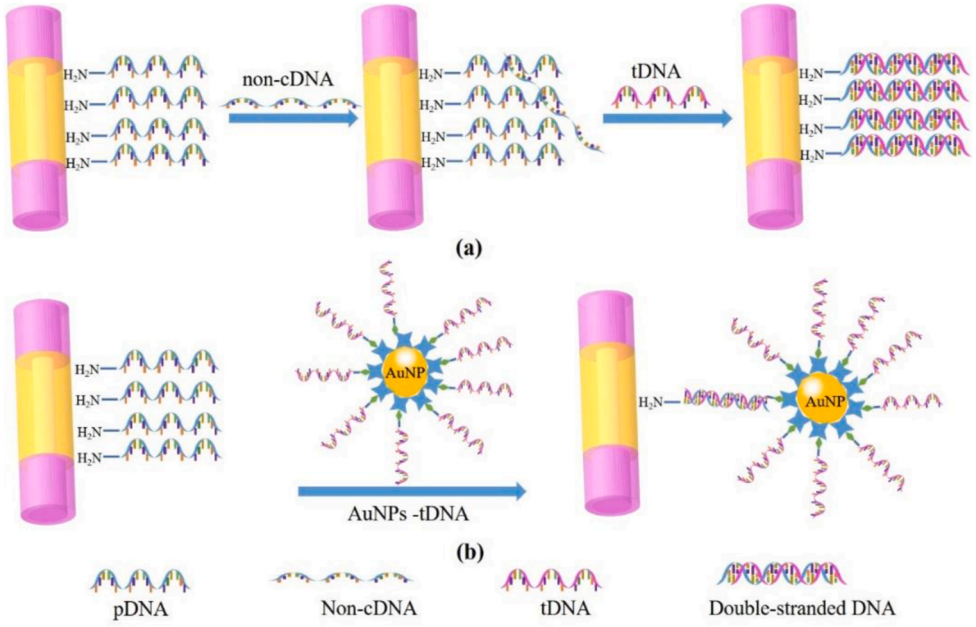

Fig. 4. (a) Common DNA hybridization detection scheme. (b) Hybridization detection scheme based on a sandwich assay amplified by AuNPs.

was centrifuged at 9000 rpm for 10 min, and then the supernatant (containing the tDNA molecules that were not successfully modified on the AuNPs) was removed, and the precipitate was resuspended in PBS buffer. At this time, tDNA has been successfully modified on AuNPs.

In order to verify that streptavidin molecules do bind to AuNPs in the above process, two comparative experiments were performed.

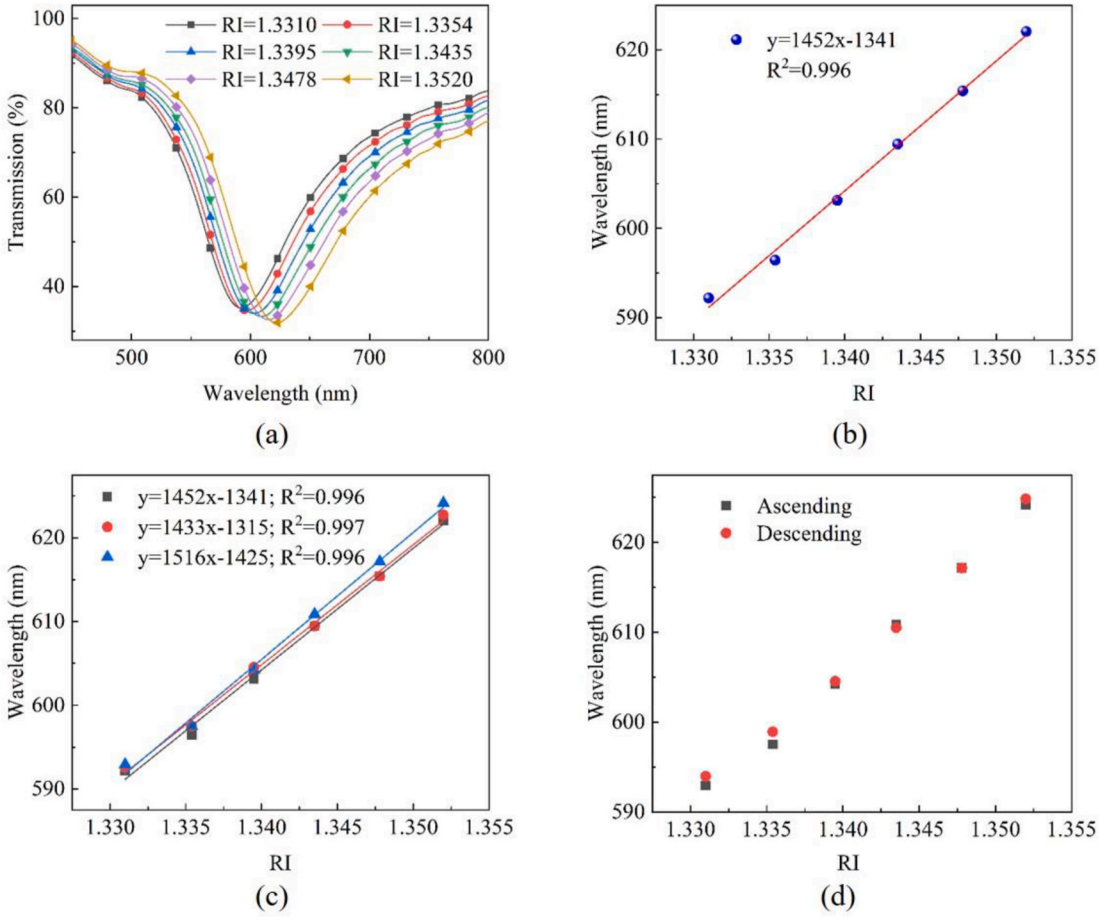

Fig. 5. RI measurement experiment of MMF-HCF-MMF structure (a) SPR spectrum shift under salt solutions with different RI. (b) RI sensitivity fitting. (c) Repeatability test under different salt solutions. (d) Hysteresis test.

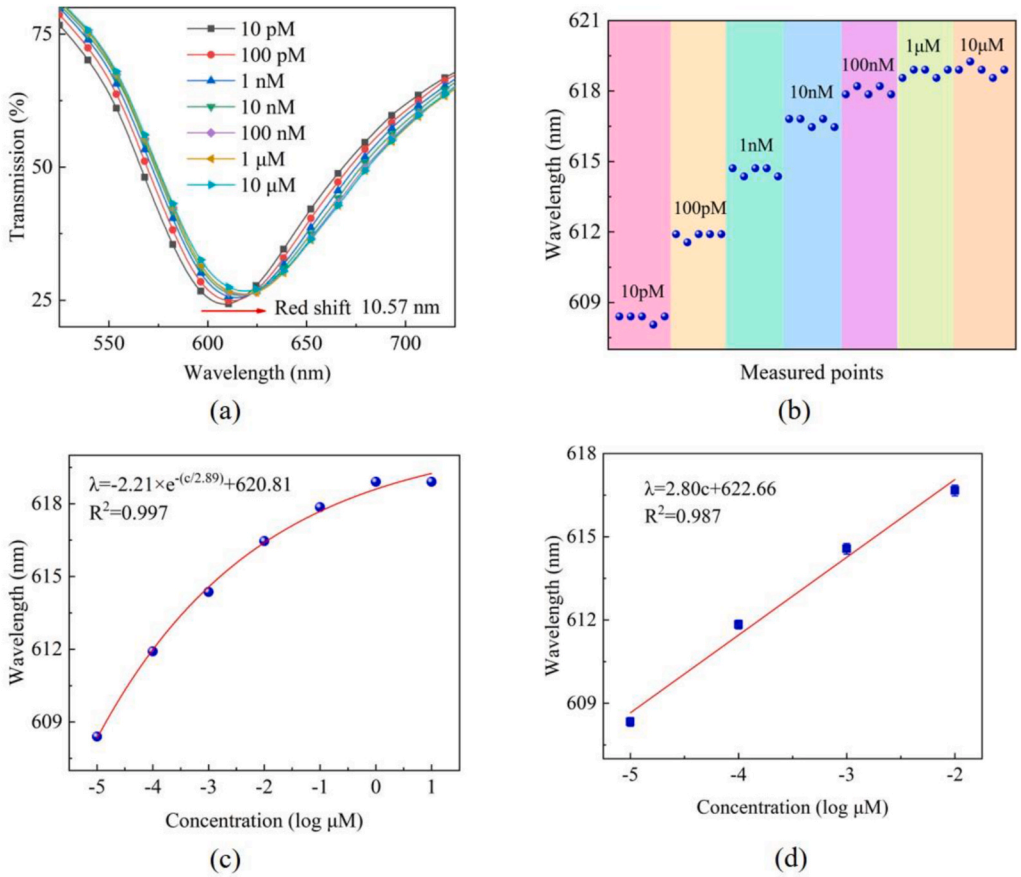

Fig. 6. (a) SPR spectrum after the tDNA and the pDNA have hybridized and stabilized. (b) Resonance wavelength fluctuations within 5 min after hybridization stabilization. (c) Logarithmic fit between the concentration of tDNA and the resonance wavelength. (d) Log-linear fitting between the concentration of the tDNA and the resonance wavelength.

Experiment 1: as shown in Fig. 3(a), the AuNPs solution prepared in the experiment was centrifuged at 9000 rpm for 20 min, and the obtained precipitation was resuspended in PBS. The final solution is black, which is attributed to the aggregation of AuNPs in high-concentration salt solution [40–42]. Experiment 2: as shown in Fig. 3(b), the mixed solution of streptavidin and AuNPs after incubation was centrifuged, and the obtained precipitate was resuspended in PBS. The final solution still showed red. We speculate that this is because the streptavidin on the surface of AuNPs prevents the aggregation of AuNPs in the salt solution. Therefore, these two control experiments show that streptavidin has been successfully modified on AuNPs.

3.4. Two DNA hybridization schemes

As shown in Fig. 2, after the pDNA is functionalized on the optical fiber sensing area, DNA hybridization detection will be performed. In this paper, in order to improve the detection sensitivity, two DNA hybridization detection schemes are designed. The first is the common DNA hybridization scheme, as shown in Fig. 4(a). Different concentrations of tDNA solutions or non-cDNA solutions hybridize with pDNA on the surface of the fiber to achieve the recognition of specific DNA sequences. The second is a sandwich analysis scheme based on AuNPs amplification, as shown in Fig. 4(b). First, biotin-tDNA or non-cDNA at different concentrations are immobilized on AuNPs as described in section 3.3, and then they are hybridized with pDNA on the surface of the optical fiber.

4. Results and discussion

4.1. RI measurement

Before DNA hybridization detection, the RI sensitivity of the MMF-HCF-MMF structure was measured through a series of salt solutions with different concentrations. The results of RI measurement are shown in Fig. 5. It can be seen that the structure has a high RI sensitivity of 1452 nm/RIU, which ensures that the structure can be used for highly sensitive DNA hybridization detection. Fig. 5(c and d) show the test results of the repeatability and hysteresis of the structure. The good repeatability and hysteresis characteristics of the sensor ensure that the sensor can work stably and reliably in detecting DNA hybridization.

4.2. Common DNA hybridization detection experiment

The optical fiber SPR sensor proposed in this paper has high RI sensitivity, so it has the ability to detect DNA hybridization. After immobilizing 1 μM pDNA on the sensing area, a series of different concentrations of tDNA (10 pM, 100 pM, 1 nM, 10 nM, 100 nM, 1 μM and 10 μM), were pumped into the sensing region and hybridized with pDNA. During this process, the spectrum exhibited a significant red shift, and then gradually stabilized. This is attributed to the tDNA being captured by the pDNA, which causes an increase in RI on the surface of the optical fiber. When the hybridization between the pDNA and the tDNA at a certain concentration reached an equilibrium state, the spectrum remained stable and no longer moved. After the spectrum stabilized, we recorded the spectrum every minute for a total of 5 min to confirmed that the sensor's spectrum had indeed stabilized. After that,

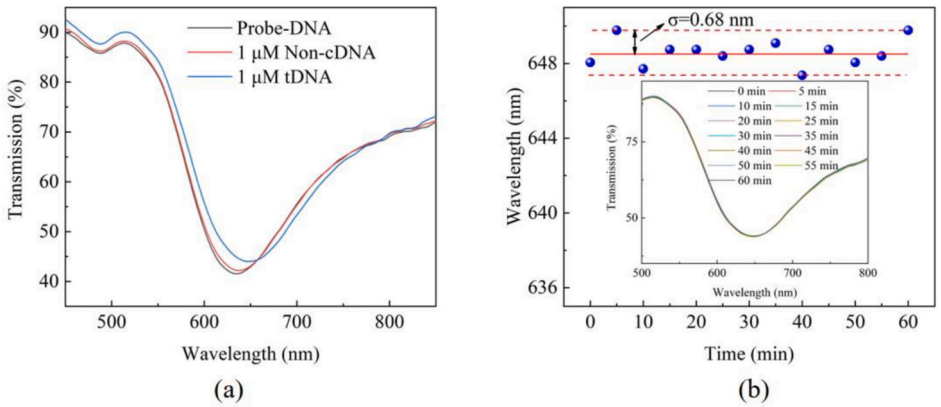

Fig. 7. (a) Specificity test results. (b) Stability test results within 1 h after DNA hybridization.

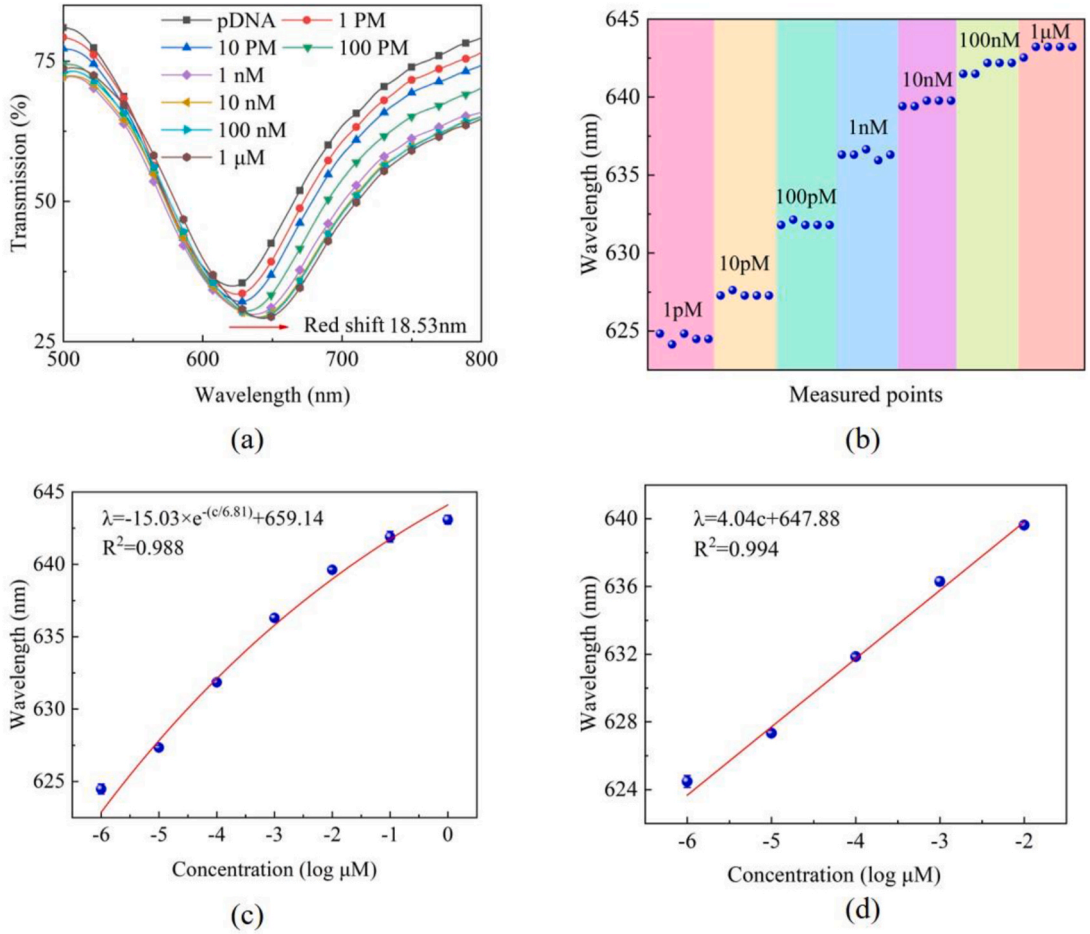

Fig. 8. (a) SPR spectra of different concentrations of tDNA modified on AuNPs. (b) Resonance wavelength fluctuations within 5 min after hybridization stabilization. (c) Logarithmic fit between the concentration of tDNA and the resonance wavelength. (d) Log-linear fitting between the concentration of the tDNA and the resonance wavelength.

the tDNA was pumped out of the microfluidic cell, and ultrapure water was pumped in to wash the unbound or weakly bound tDNA in the sensing area. After the ultrapure water was discharged, the next concentration of tDNA could be detected.

Fig. 6(a) shows the spectra after the target DNA and pDNA on the surface of the fiber are hybridized and stabilized. It can be seen from the figure that as the tDNA concentration increases, the spectrum gradually red-shifts. When the concentration of the tDNA reaches 10 μM, the spectrum shift is very weak. This is because the binding between the pDNA and the tDNA has reached saturation, and then the spectrum almost no longer redshifts even if the concentration of the tDNA is increased. For each DNA concentration hybridization, the relationship between the fluctuation of resonance wavelength recorded within 5 min after spectral stability and concentration is shown in Fig. 6(b). After that, the average value of the resonance wavelength of the stabilized spectrum and the concentration are used for logarithmic fitting, and the fitting result is shown in Fig. 6(c). It can be seen from Fig. 6(c) that the tDNA concentration increases from 10 pM to 10 μM and the spectrum

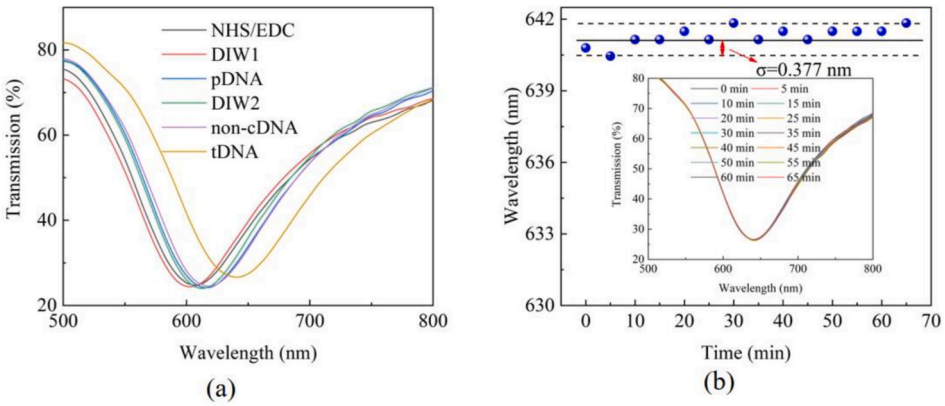

Fig. 9. (a) Specific test. (b) Stability test results within 65 min.

Table 1
Performance comparison of different types of optical fiber DNA sensors.

Structure	Mechanical strength	Detection range	Detection limit	Ref.
Microfiber Sagnac interferometer	Fragile	100 pM-1 μM	75 pM	[16]
D-shape fiber SPR based on graphene/Au film	Robust	100 pM-1 μM	100 pM	[17]
WGM resonator based on grapefruit-MOF	Fragile	10 pM-100 nM	10 pM	[19]
Reflective microfiber probe	Fragile	10 pM-100 nM	10 pM	[20]
No-core fiber SPR and MZI	Robust	–	80 nM	[25]
Unclad fiber LSPR	Fragile	100 pM-1 μM	67 pM	[31]
Tapered optical fiber MZI	Fragile	0.1 fM-100 pM	0.1 fM	[45]
Hollow core fiber SPR + AuNPs amplification	Robust	1 pM-10 nM	1 pM	This work

Table 2
Comparison of sensitization effect of fiber optic SPR biosensor.

SPR sensing structure	Analyte	Sensitization method	Sensitization effect	Operation difficulty	Ref.
MMF-PCF-MMF	IgG	Inserting graphene oxide on Au film	RI sensitivity improved to 1.68 times	Low	[27]
MMF-SMF-MMF	RI	Inserting Ti_3C_2Tx Mxene on Au film	RI sensitivity improved to 1.30 times	High	[28]
U-shaped fiber	IgG	Inserting MoS_2 nanosheets between metal film and fiber	RI sensitivity improved to 1.59 times	High	[29]
MMF-HCF-MMF	tDNA	Amplification with tDNA functionalized AuNPs	Signal response improved to 1.75 times	Low	This work

shifts a total of 10.57 nm. The concentration from 10 pM to 10 nM is log-linearly fitted with the resonance wavelength, as shown in Fig. 6(d), which indicates that the DNA biosensor has a detection sensitivity of 2.80 nm/Log(μM) in the range of 10 pM-10 nM.

After that, in order to confirm the recognition ability of the sensor for specific DNA sequences, we performed a set of specific test experiments. 1 μM non-cDNA and 1 μM tDNA were pumped into the optical fiber sensing area where pDNA had been immobilized, and then the stabilized spectra were recorded separately, as shown in Fig. 7(a). Compared with tDNA, the spectrum shift caused by the binding of non-cDNA and pDNA is very weak, which proves that the sensor can specifically recognize tDNA sequences. After the binding of 1 μM tDNA and pDNA was stable, we monitored the stability of the sensor within 1 h by recording the spectrum every 5 min. The results of stability test are shown in Fig. 7(b). The standard deviation of the wavelength fluctuation within 1 h is 0.68 nm, which confirms that the sensor has good stability.

4.3. DNA hybridization detection based on AuNPs amplification

To further improve the detection sensitivity and detection limit of the sensor, we carried out DNA hybridization detection based on AuNPs sensitization. The detection scheme is shown in Fig. 4(b). In brief, a series of different concentrations of tDNA modified on AuNPs are sequentially pumped into the sensing region, and the movement of the SPR spectrum is recorded. The specific experimental operation process is the same as that in section 4.2, and will not be described in detail here. The experimental results obtained are shown in Fig. 8. Fig. 8(a) shows that as the tDNA concentration increases, the spectrum gradually red-shifts. The redshift of the whole process is 18.53 nm, which is 1.75 times of the redshift without AuNPs sensitization.

Here, the signal amplification achieved by AuNPs is mainly attributed to two aspects. On the one hand, the electromagnetic coupling effect between the AuNPs and the gold film. On the other hand, the large mass ratio of AuNPs increases the RI on the surface of the optical fiber [36,43,44]. Fig. 8(c) shows the logarithmic fit between the tDNA of each concentration and the mean resonance wavelength. The first 5 points in the curve fitting are taken for log-linear fitting, as shown in Fig. 8(d). The DNA hybridization sensor enhanced by AuNPs has a linear detection range of 1 pM–10 nM and a detection sensitivity of 4.04 nm/log(μM).

Then, based on the AuNPs enhancement protocol, the specificity and stability of the sensor were tested. The test results are shown in Fig. 9(a) and Fig. 9(b). Compared with tDNA, the spectrum shift caused by the binding of non-cDNA is insignificant, which indicates that the sensor has the ability to recognize specific DNA sequences. After DNA hybridization, the standard deviation of the resonance wavelength fluctuation was 0.377 nm within 65 min, which indicated that the sensor had the ability to operate stably for a long time.

Table 1 compares the proposed sensing performances with other proposed sensors, including the structure mechanical strength, detection range and detection limit. As can be seen from Table 1, the detection limit of the proposed optical fiber DNA sensor based on Au NPs amplification is lower than that of most of the proposed sensors, and it has the advantages of high mechanical strength and wide detection range. Besides, Table 2 compares the sensitization effect of this sensitization scheme with that of other fiber SPR biosensors. It can be seen that the sensitization scheme proposed in this paper has the advantages of simple operation and good sensitization effect.

5. Conclusion

In this paper, a DNA hybridization detection scheme based on AuNPs enhancement has been proposed and experimentally confirmed with good specificity and stability. The main innovation of this paper is to demonstrate the feasibility of Au NPs sensitization when measuring DNA by optical fiber SPR sensor. To facilitate binding of Au NPs, biotinylated DNA was directly tested. In fact, on the basis of verifying the feasibility of this sensitization method, this method can be used to detect any DNA with high sensitivity, such as deafness gene, the COVID-19 gene and lung cancer gene, etc. Experimental results indicate that the minimum detectable concentration of the sensor is as low as 1 pM, which is betterer than most existing fiber-optic DNA sensors, giving the sensor the potential for low-concentration or small-fragment DNA detection.

Credit author statement

Like Li: Methodology, Investigation, Writing – original draft preparation. **Ya-nan Zhang:** Conceptualization, Funding acquisition. **Wanlu Zheng:** Validation, Data curation. **Xuegang Li:** Writing- Reviewing and Editing. **Yong Zhao:** Resources, Supervision.

Declaration of competing interest

The authors declare that they have no known competing financial interests or personal relationships that could have appeared to influence the work reported in this paper.

Acknowledgments

This work was supported in part by the National Natural Science Foundation of China under Grant 62075036, the National Natural Science Foundation of Liaoning Province under Grant 2020-YQ-04, the Fundamental Research Funds for the Central Universities under Grants N2104019 and N2002019, the State Key Laboratory of Alternate Electrical Power System with Renewable Energy Sources under Grant LAPS20020, State Key Laboratory of Synthetical Automation for Process Industries under Grant 2013ZCX09, Hebei Natural Science Foundation under Grant No. F2020501040.

References

[1] M. Makela, P.T. Lin, Detection of SARS-CoV-2 DNA targets using femtoliter optofluidic waveguides, Anal. Chem. 93 (9) (2021) 4154–4159.
[2] M. Janik, S.V. Hamidi, M. Koba, et al., Real-time isothermal DNA amplification monitoring in picoliter volumes using an optical fiber sensor, Lab Chip 21 (2) (2021) 397–404.
[3] S. Goltry, N. Hallstrom, T. Clark, et al., DNA topology influences molecular machine lifetime in human serum, Nanoscale 7 (23) (2015) 10382–10390.
[4] Y. Huang, M. Tao, S. Luo, et al., A novel nest hybridization chain reaction based electrochemical assay for sensitive detection of circulating tumor DNA, Anal. Chim. Acta 1107 (2020) 40–47.
[5] T.L. Tran, T.X. Chu, P.Q. Do, et al., In-channel-grown polypyrrole nanowire for the detection of DNA hybridization in an electrochemical microfluidic biosensor, J. Nanomater. 458629 (2015).
[6] L. Shuang, X. Shang, L. Jia, et al., A universal colorimetry for nucleic acids and aptamer-specific ligands detection based on DNA hybridization amplification, Anal. Biochem. 528 (2017) 47–52.
[7] E. Tan, J. Wong, D. Nguyen, et al., Isothermal DNA amplification coupled with DNA nanosphere-based colorimetric detection, Anal. Chem. 77 (24) (2005) 7984–7992.
[8] B.A. Prabowo, A. Purwidyantri, B. Liu, et al., Gold nanoparticle-assisted plasmonic enhancement for DNA detection on a graphene-based portable surface plasmon resonance sensor, Nanotechnology 32 (9) (2020), 095503.
[9] L. He, M.D. Musick, S.R. Nicewarner, et al., Colloidal Au-enhanced surface plasmon resonance for ultrasensitive detection of DNA hybridization, J. Am. Chem. Soc. 122 (38) (2000) 9071–9077.
[10] M. Fan, G.F. Andrade, A.G. Brolo, A review on recent advances in the applications of surface-enhanced Raman scattering in analytical chemistry, Anal. Chim. Acta 1097 (2020) 1–29.
[11] J. Hu, C.Y. Zhang, Sensitive detection of nucleic acids with rolling circle amplification and surface-enhanced Raman scattering spectroscopy, Anal. Chem. 82 (21) (2010) 8991–8997.
[12] M. Barozzi, A. Manicardi, A. Vannucci, et al., Optical fiber sensors for label-free DNA detection, J. Lightwave Technol. 35 (16) (2016) 3461–3472.
[13] X. Li, N. Chen, X. Zhou, et al., A review of specialty fiber biosensors based on interferometer configuration, J. Biophot. (2021), e202100068.
[14] L. Li, Y.N. Zhang, Y. Zhou, et al., Optical Fiber Optofluidic Bio-chemical Sensors: A Review, Laser Photonics Rev., 2021, p. 2000526.
[15] Y. Liu, X. Li, Y.N. Zhang, et al., Fiber-optic sensors based on Vernier effect, Measurement 167 (2021) 108451.
[16] S. Gao, L.P. Sun, J. Li, et al., High-sensitivity DNA biosensor based on microfiber Sagnac interferometer, Opt Express 25 (12) (2017) 13305–13313.
[17] W. Gong, S. Jiang, Z. Li, et al., Experimental and theoretical investigation for surface plasmon resonance biosensor based on graphene/Au film/D-POF, Opt Express 27 (3) (2019) 3483–3495.
[18] D.S. Rivero, A. Urrutia, C. Ruiz-Zamarreño, et al., Advances in fiber optic DNA-based sensors: a review, IEEE Sensor. J. 21 (11) (2020) 12679–12691.
[19] Y. Wang, H. Zhang, S. Duan, et al., Label-free in-situ detection for DNA hybridization employing grapefruit-microstructured-optical-fiber-based microfluidic whispering gallery mode resonator, IEEE Sensor. J. 21 (7) (2020) 9148–9154.
[20] Y. Li, F. Fang, L. Yang, et al., In-situ DNA hybridization detection based on a reflective microfiber probe, Opt Express 28 (2) (2020) 970–979.
[21] L. Liang, L. Jin, Y. Ran, et al., Interferometric detection of microRNAs using a capillary optofluidic sensor, Sensor. Actuator. B Chem. 242 (2017) 999–1006.
[22] B. Song, H. Zhang, B. Liu, et al., Label-free in-situ real-time DNA hybridization kinetics detection employing microfiber-assisted Mach-Zehnder interferometer, Biosens. Bioelectron. 81 (2016) 151–158.
[23] Y. Zhao, R.J. Tong, F. Xia, et al., Current status of optical fiber biosensor based on surface plasmon resonance, Biosens. Bioelectron. 142 (2019) 111505.
[24] L. Li, Y.N. Zhang, Fiber-optic SPR pH sensor based on MMF-NCF-MMF structure and self-assembled nanofilm, IEEE Trans. Instrum. Meas. 70 (2020) 1–9.
[25] P. Gong, Y. Wang, X. Zhou, et al., In situ temperature-compensated DNA hybridization detection using a dual-channel optical fiber sensor, Anal. Chem. 93 (2021) 10561–10567.
[26] S. Zeng, D. Baillargeat, H.P. Ho, et al., Nanomaterials enhanced surface plasmon resonance for biological and chemical sensing applications, Chem. Soc. Rev. 43 (10) (2014) 3426–3452.
[27] Q. Wang, B. Wang, Sensitivity enhanced SPR immunosensor based on graphene oxide and SPA co-modified photonic crystal fiber, Opt Laser. Technol. 107 (2018) 210–215.
[28] Y. Chen, Y. Ge, W. Huang, et al., Refractive index sensors based on Ti3C2Tx MXene fibers, ACS Appl. Nano Mater. 3 (1) (2020) 303–311.
[29] H. Song, Q. Wang, W. Zhao, A novel SPR sensor sensitivity-enhancing method for immunoassay by inserting MoS2 nanosheets between metal film and fiber, Opt Laser. Eng. 132 (2020) 106135.
[30] F. Xia, H. Song, Y. Zhao, et al., Ultra-high sensitivity SPR fiber sensor based on multilayer nanoparticle and Au film coupling enhancement, Measurement 164 (2020) 108083.
[31] M. Lu, W. Peng, M. Lin, et al., Gold nanoparticle-enhanced detection of DNA hybridization by a block copolymer-templating fiber-optic localized surface plasmon resonance biosensor, Nanomaterials 11 (3) (2021) 616.
[32] S. Jia, C. Bian, J. Sun, et al., A wavelength-modulated localized surface plasmon resonance (LSPR) optical fiber sensor for sensitive detection of mercury (II) ion by gold nanoparticles-DNA conjugates, Biosens. Bioelectron. 114 (2018) 15–21.
[33] H. Yuan, G. Sun, W. Peng, et al., Thymine-functionalized gold nanoparticles (Au NPs) for a highly sensitive fiber-optic surface plasmon resonance mercury ion nanosensor, Nanomaterials 11 (2) (2021) 397.
[34] L. Zhang, Y. Tang, L. Tong, Micro-/nanofiber optics: merging photonics and material science on nanoscale for advanced sensing technology, iScience 23 (1) (2020) 100810.
[35] M.J. Yin, B. Gu, Q.F. An, et al., Recent development of fiber-optic chemical sensors and biosensors: mechanisms, materials, micro/nano-fabrications and applications, Coord. Chem. Rev. 376 (2018) 348–392.
[36] H. Qian, Y. Huang, X. Duan, et al., Fiber optic surface plasmon resonance biosensor for detection of PDGF-BB in serum based on self-assembled aptamer and antifouling peptide monolayer, Biosens. Bioelectron. 140 (2019) 111350.
[37] A. Bertucci, A. Manicardi, A. Candiani, et al., Detection of unamplified genomic DNA by a PNA-based microstructured optical fiber (MOF) Bragg-grating optofluidic system, Biosens. Bioelectron. 63 (2015) 248–254.
[38] G. Liang, Z. Zhao, Y. Wei, et al., Plasma enhanced label-free immunoassay for alpha-fetoprotein based on a U-bend fiber-optic LSPR biosensor, RSC Adv. 5 (31) (2015) 23990–23998.
[39] M. Lu, L. Hong, Y. Liang, et al., Enhancement of gold nanoparticle coupling with a 2D plasmonic crystal at high incidence angles, Anal. Chem. 90 (11) (2018) 6683–6692.
[40] Z. Luo, J. Zhang, Y. Wang, et al., An aptamer based method for small molecules detection through monitoring salt-induced AuNPs aggregation and surface plasmon resonance (SPR) detection, Sensor. Actuator. B Chem. 236 (2016) 474–479.
[41] H. Li, L.J. Rothberg, Label-free colorimetric detection of specific sequences in genomic DNA amplified by the polymerase chain reaction, J. Am. Chem. Soc. 126 (35) (2004) 10958–10961.
[42] S. Zhou, Y. Gan, L. Kong, et al., A novel portable biosensor based on aptamer functionalized gold nanoparticles for adenosine detection, Anal. Chim. Acta 1120 (2020) 43–49.

[43] M. Loyez, M. Lobry, E.M. Hassan, et al., HER2 breast cancer biomarker detection using a sandwich optical fiber assay, Talanta 221 (2021) 121452.
[44] M. Frasconi, C. Tortolini, F. Botre, et al., Multifunctional Au nanoparticle dendrimer-based surface plasmon resonance biosensor and its application for improved insulin detection, Anal. Chem. 82 (17) (2010) 7335–7342.
[45] N. Zainuddin, H. Chee, M. Ahmad, et al., Sensitive Leptospira DNA detection using tapered optical fiber sensor, J. Biophot. 11 (8) (2018), e201700363.